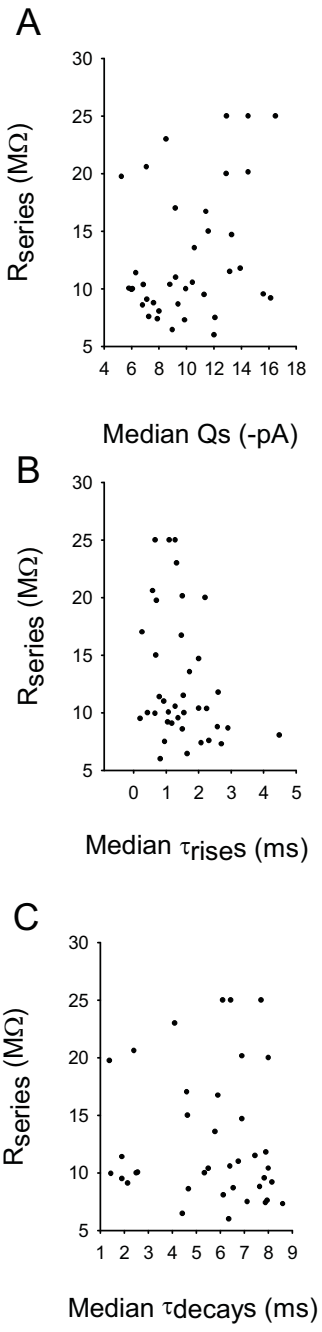
A
30
25
20
15
10
5
R_{series} (MΩ)
4 6 8 10 12 14 16 18
Median Qs (-pA)
B
30
25
20
15
10
5
R_{series} (MΩ)
0 1 2 3 4 5
Median τ_{rises} (ms)
C
30
25
20
15
10
5
R_{series} (MΩ)
1 2 3 4 5 6 7 8 9
Median τdecays (ms)

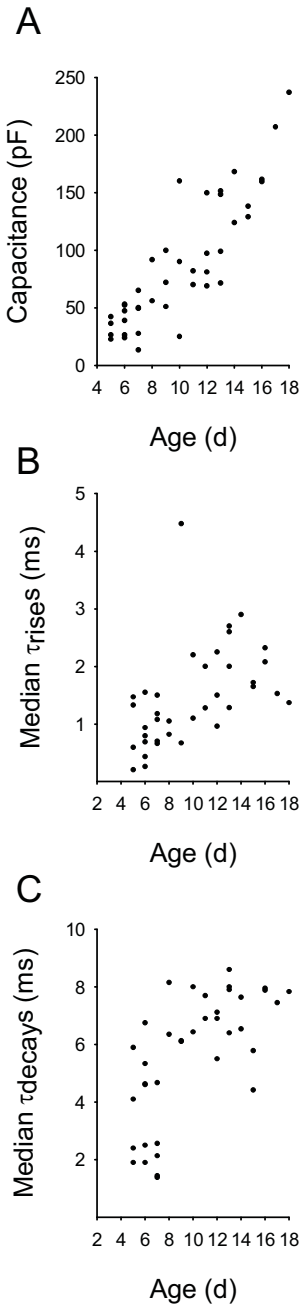
A
Capacitance (pF)
0
50
100
150
200
250
4 6 8 10 12 14 16 18
Age (d)
B
Median τrises (ms)
1
2
3
4
5
2 4 6 8 10 12 14 16 18
Age (d)
C
Median τdecays (ms)
2
4
6
8
10
2 4 6 8 10 12 14 16 18
Age (d)

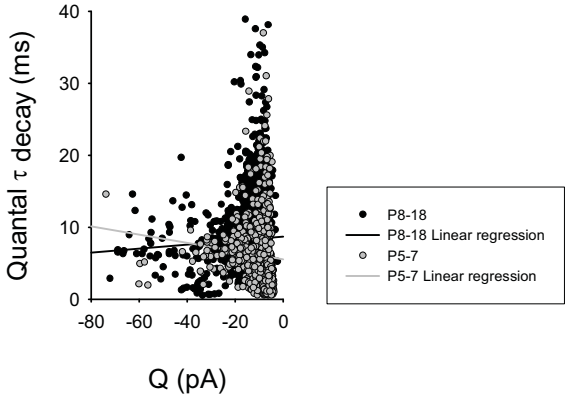
Quantal τ decay (ms)
40
30
20
10
0
-80
-60
-40
-20
0
Q (pA)
P8-18
P8-18 Linear regression
P5-7
P5-7 Linear regression

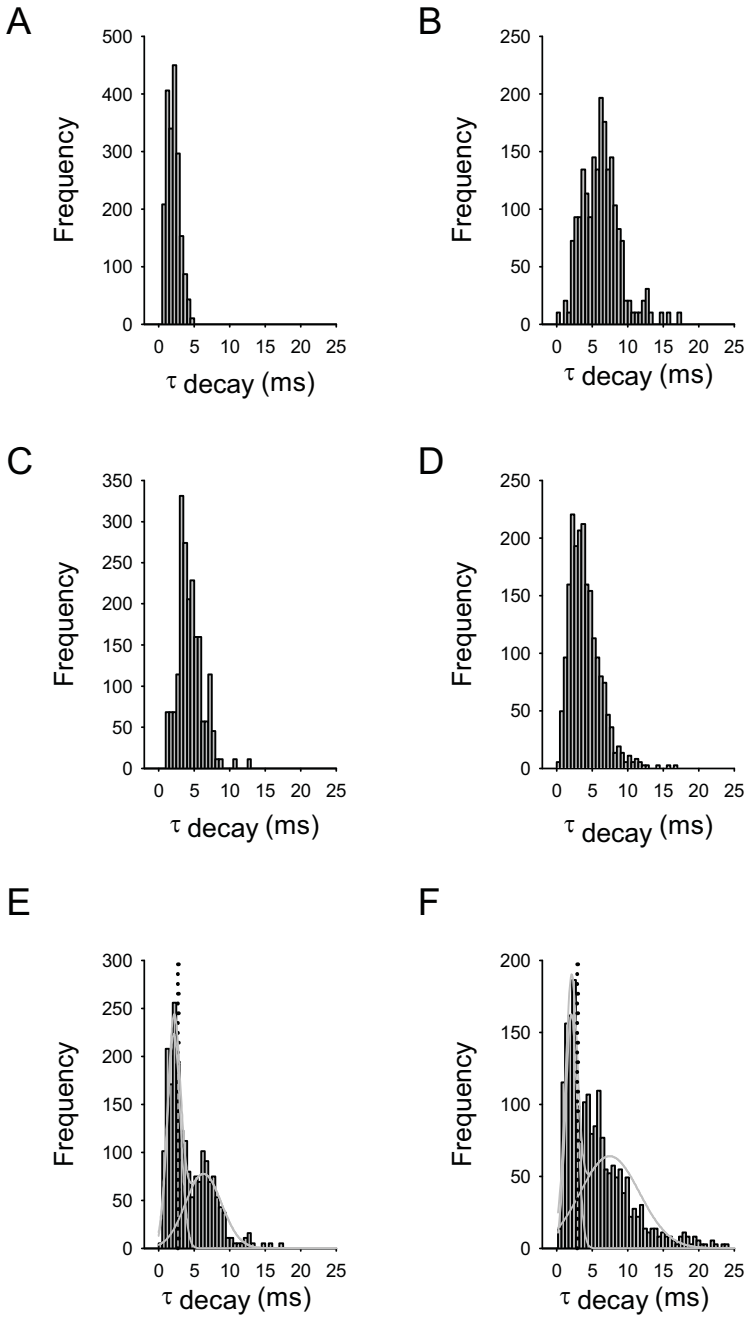
A
B
C
D
E
F
Frequency
τ decay (ms)
0
5
10
15
20
25

Supplemental Figure 1: AMPAR-mediated Q, τ_{rise}, and τ_{decay} were independent of series resistance. A. Median Qs did not correlate with series resistance (n=38). B. Median τ_{rise}s were unaffected by series resistances recorded (n=38). C. Median τ_{decay}s were unaffected by series resistances recorded (n=38).

Supplemental Figure 2: Only AMPAR-mediated τ_{rise} was affected by filtering. A. Cell capacitance, an estimate of cell size, increased steadily during the developmental window examined from P5-18 (n=38). B. Similar to cell capacitance, median τ_{rise}s steadily increased with development (n=38), suggesting that these parameters were related. C. Scatter plot of median τ_{decay}s across all developmental time points P5-P18 also showed an opposing relationship compared to age and, therefore, cell capacitance, suggesting that median τ_{decay}s were not influenced by cell capacitance and likely filtering in the same way as median τ_{rise}s.

Supplemental Figure 3. Correlation of quantal amplitudes (Q) and quantal τ_{decay} for individual, pooled events at P5-7 and P8-18. Quantal τ_{decay} and Q (732 events) pooled from neurons (n = 15) at P5-7 were plotted (grey circles) and compared to P8-18 (1985 events, n = 23 neurons, black circles) to determine whether these two parameters were related. Q and quantal τ_{decay} did not appear correlated at either age based on regression lines for events at P5-7 (grey line, $r^2 = 0.0027$) and P8-18 (black line, $r^2 = 0.0015$).

Supplemental Figure 4. Modeling sources of variability of CV τ_{decay} to demonstrate that distinct synapses with different kinetics best describe experimental distributions of quantal τ_{decay}. AMPARs were modeled with a detailed macroscopic kinetic scheme (67). Rate constants and channel conductances for AMPARs were as published except the closing rate (α) was adjusted to give different rates for mean quantal τ_{decay}. In order to simulate the variability of peak glutamate concentration in the synaptic cleft, it was assumed that glutamate was released from vesicles containing 80 mM glutamate with a mean radius of 17nm with a standard deviation of 7.5 nm (which is three times reported values (32) in order to maximize variability) into a synaptic cleft volume of 9 aL. The resulting exponential distribution of glutamate cleft concentrations had a mean of 0.3 mM. Stochastic AMPARs, simulated with the Monte Carlo technique as done previously (2), when activated by a glutamate pulse with a peak time of 2 μs and decay time of 1 ms, resulted in a average response τ_{decay} of 6.1 ms with $\alpha = 300s^{-1}$ and average response τ_{decay} of 2.1 ms with $\alpha = 900\ s^{-1}$. Total AMPAR numbers were fixed at 25 to result in mean simulated Q (-12 pA at -70 mV) similar to experimental results. Random noise (2 pA rms) was added to ensembles of 250-1000 modeled synaptic AMPAR responses; filtering (Gaussian low-pass of 2 kHz) did not significantly alter results. Modeled CV_Q (0.37) was similar to that found experimentally. Empiric Gaussian distributions from non-binned event data were fitted with a maximum likelihood estimator via a simplex method(72). Five different scenarios were tested in order to investigate the source of variability of quantal τ_{decay}. Responses were analyzed in a similar fashion to experimental data. A. In the first scenario, all 25 AMPARs were given $\alpha = 900\ s^{-1}$. This resulted in a $CV\tau_{decay}$ of 0.42 and a median quantal τ_{decay} of 2.0 ms (250 trials). B. In the second scenario, all 25 AMPARs were given $\alpha = 300\ s^{-1}$. This

resulted in a $CV\tau_{decay}$ of 0.44 and a median quantal τ_{decay} of 6.1 ms (250 trials). C. In the third scenario, 13 AMPARs had $\alpha = 900\ s^{-1}$ and 12 AMPARs had $\alpha = 300\ s^{-1}$. This resulted in a $CV\tau_{decay}$ of 0.40, a median quantal τ_{decay} of 4.5 ms and no nadir of separation seen (250 trials). D. In the fourth scenario, AMPAR were randomized with a uniform probability distribution to have either $\alpha = 900\ s^{-1}$ or $\alpha = 300\ s^{-1}$. As expected, this resulted in a median τ_{decay} between the distributions in (A) and (B) (3.6 ms) and did not show peaks or nadirs; however, $CV\tau_{decay}$ was increased to 0.55 (1000 trials). E. In the final scenario, the responses with $\alpha = 900\ s^{-1}$ (A) and $\alpha = 300\ s^{-1}$ (B) were pooled to simulate two independent AMPAR synapses (i.e. each activated with equal probability) with different kinetics. Peaks and a nadir appeared in the distribution of quantal τ_{decay} with median τ_{decay} of 4.2 ms and $CV\tau_{decay}$ of 0.69, similar to that seen experimentally at P5-7 (c.f. Fig. 5A). However, Hartigan's Dip test did not identify significant multimodality ($D = 018$, $p \approx 0.8$, modal break (2.7 ms) indicated by dotted line), even though the distribution appeared multimodal and was generated from two distributions. Fitted Gaussian distributions (solid grey lines) segregated 51% faster events with mean of 2.1 ms ($\sigma = 0.9$ ms) from 49% slower events with mean of 6.3 ms ($\sigma = 2.5$ ms), consistent with equal contributions from the 2 independent synapses. F. Pooled quantal τ_{decay} events from all neurons at P5-7 suggested 2 distributions but did not have a significant Dip test ($D = 0.011$, 732 events, $p \approx 0.9$, modal break (2.9 ms) indicated by dotted line). Fitted Gaussian distributions (solid grey lines) segregated 33% faster events with mean of 2.1 ms ($\sigma = 0.8$ ms) from 67% slower events with mean of 7.5 ms ($\sigma = 4.2$ ms). If there are 2 synapse types, "faster" and "slower", with equal release probabilities (c.f. Fig. 2A,B), this suggest that approximately 30% of activated synapses at P5-7 are distinct and "faster".